INTEGRATED OPTICAL COMPONENTS FOR WDM OPTICAL/WIRELESS APPLICATIONS.

L.A. Johansson, J.S. Barton, M.L. Mašanović, J.M. Hutchinson, J.A. Henness,
Y.A. Akulova*, G.A. Fish* and L.A. Coldren

Department of Electrical and Computer Engineering
University of California, Santa Barbara, CA 93106
Tel: (805) 893-4543, Fax: (805) 893-7500, email: leif@ece.ucsb.edu
*Agility Communications, Inc., 600 Pine Ave, Santa Barbara, CA 93117

Abstract – High-performance, widely tunable MZ and EA modulated analog transmitters suited for WDM optical/wireless applications are overviewed. Further, the potential to use monolithically integrated wavelength converters for these applications is also investigated.

I. Introduction

Wireless over fiber has been proposed to increase capacity of wireless systems and system flexibility, both in terms of transparency of modulation format and flexible allocation of spectrum resources [1]. As wireless systems moves from single-service narrowband applications to multi-service broadband applications, wireless over fiber can also preserve relatively low-complexity and small size of antenna base stations. The merging of WDM and wireless over fiber technologies will further enhance system reconfigurability and capacity [2]. A major challenge involving WDM wireless over fiber systems is for the individual components to deliver sufficient performance to transmit broadband wireless signals up to the order of 1 GHz bandwidth or SCM multiservice signals, without significant degradation of signal fidelity. This in addition to be compatible with a reconfigurable WDM environment and transmission of digital data. This challenge is enhanced by the need to cascade several components to form the complete link, possibly involving switching or wavelength conversion in the process. This presentation will review current efforts to produce high-performance integrated components for WDM analog systems, such as widely tunable transmitters and wavelength converters capable of converting any λ_{in} to any λ_{out} within a specified band.

II. SG-DBR laser platform

The devices used for the work described within this paper are based on widely tunable SG-DBR lasers. The SG-DBR laser includes gain and phase sections positioned between two “sampled grating” distributed reflectors, sampled at different periods such that only one of their multiple reflection peaks can coincide at a time [3]. An offset quantum-well structure provides a platform for integration of the laser with other active regions, such as detectors or semiconductor optical amplifiers (SOA), and passive regions, such as phase or amplitude modulators. Typical performance of an SG-DBR laser integrated to an SOA is more than 10mW output power, lower than 2 MHz linewidth, and more than 40 dB sidemode suppression ratio over more than 40 nm wavelength tuning range [4]. Despite the added SOA noise, the RIN is less than -150 dB/Hz over the entire frequency range and as low as -160 dB/Hz at 1 to 2 GHz, for more than 140 mA gain section bias, as illustrated by Fig. 1.

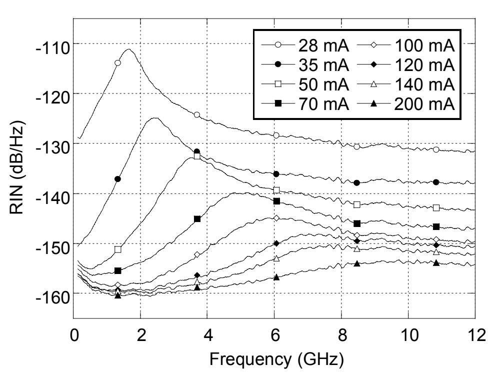

Fig. 1: Detected SGDBR-SOA RIN spectra at 1552 nm for different values of gain section bias. SOA bias is fixed at 180 mA.

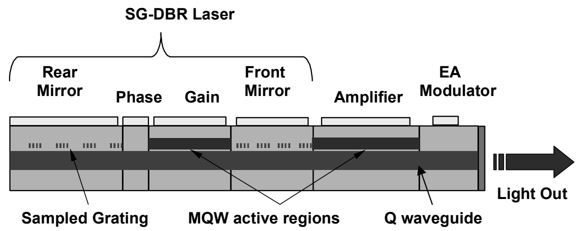

Fig 2. SGDBR-SOA-EAM Device Schematic

III. EA transmitter

Figure 2. shows the layout of an SG-DBR laser, integrated to an SOA and a Franz-Keldysh type electroabsorption modulator. The modulator uses the same bulk quaternary waveguide as the tuning sections of the laser. The Franz-Keldysh effect in the bulk waveguide material provides for larger spectral bandwidth as compared to the quantum-confined Stark effect. The bulk design allows improved power handling of the device, avoiding carrier pileup problems, up to a limit determined by Joule-heating of the device, on the order of 200mW *I-V* product, *I* being the EAM photocurrent. This combined with efficient coupling to the SOA and laser, removing any risk of input facet damage as a result of integration, allows very high power operation of the EAM. At –3V bias voltage, up to 70mA linear photocurrent has been observed.

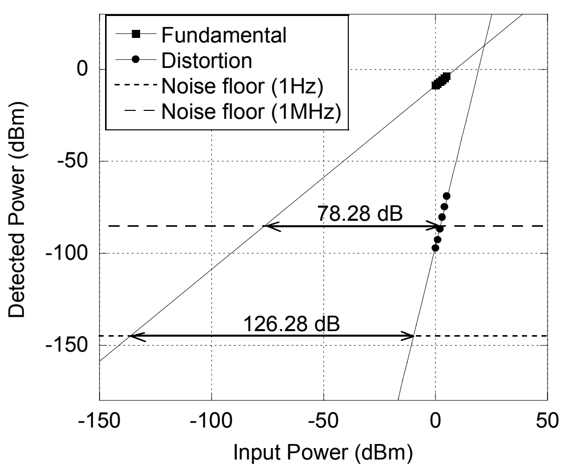

Fig. 3: Measured power of noise floor, fundamental, second and third order intermodulation products at 1552 nm, for 0 dBm to 5 dBm input RF power, 0.96mW optical power and –2.5V EAM bias. Sub-octave spurious-free dynamic range is also shown in 1Hz and 1MHz bandwidth.

The low RIN and high optical power results in a high spurious-free dynamic range, despite the relatively non-linear response of the EA-modulator. Biasing the modulator at the third order infliction point, the odd-order intermodulation products becomes determined by fifth order distortion, resulting in a sub-octave SFDR of 126.3 $dBHz^{4/5}$, illustrated by Fig. 3. The maximum broadband SFDR is found at maximum slope sensitivity and is limited by second order distortion at 97.2 $dBHz^{2/3}$ [5].

IV. MZ transmitter

The Mach-Zehnder modulator has a number of advantages compared to EA modulators. First of all, the RF link gain of a EA modulated optical link becomes limited by the absorbed photocurrent. MZ modulators do not have this limitation, being based on interferometric modulation. Second, by choosing inverting, non-inverting or a combined push-pull modulation, the modulator chirp can be controlled from positive to negative values. In terms of linearity, Mach Zehnder modulators have one disadvantage. With its sinusoidal response, the third order infliction points appear at the same bias point as zero slope sensitivity, limiting the available sub-octave SFDR.

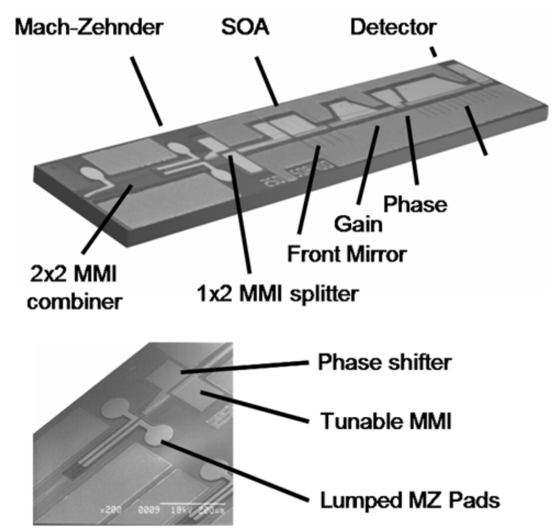

Fig. 4: MZ-SOA-SGDBR device layout

Figure 4 shows the layout of a Mach-Zehnder modulator integrated to an SG-DBR laser and an SOA [6]. In addition to RF electrodes in the arms of the MZ modulator, a phase shifter is located in one of the modulator arms. In addition to changing the phase, the bulk material in the modulator electrodes also changes the amplitude with applied voltage. The phase tuning section provides the extra degree of freedom needed to match both the amplitude and phase of the arms for full extinction at the output. The combination of phase and amplitude modulation in the arms also provides a deviation from the sinusoidal response of a typical MZ modulator. As a result, the third order infliction point no longer coincides with zero slope sensitivity, as illustrated in Fig. 5 where the power of fundamental and distortion is plotted. It is seen that at minimum third order distortion, the fundamental is less than two dB lower than at maximum slope sensitivity. At this point, the sub-octave SFDR is fifth order limited at 115 $dBHz^{4/5}$.

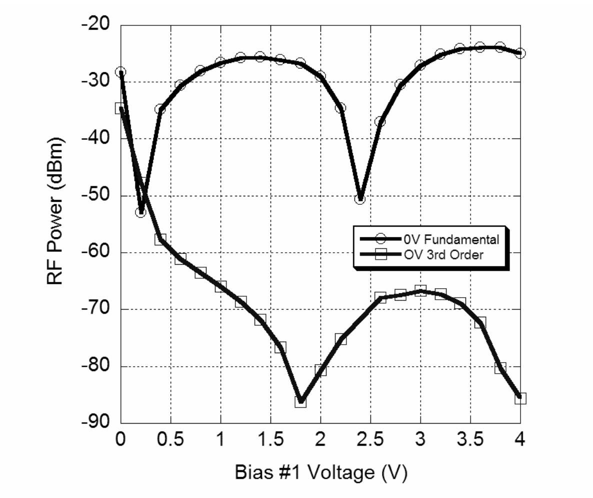

Fig. 5. Fundamental and 3^{rd} order power as a function of first electrode bias and 0V bias on second electrode.

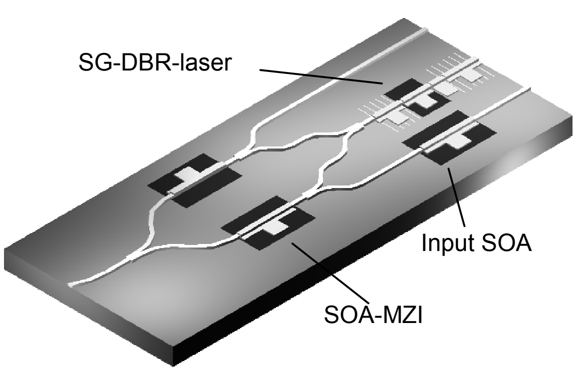

Fig. 6. Tunable all-optical wavelength converter (TAO-WC)

V. Wavelength converters

By using an input optical signal to regulate the output from an SG-DBR laser, a tunable wavelength converter is formed. Figure 6 shows an all-optical variety of this type of device. The device consists of an SG-DBR laser integrated to an SOA Mach-Zehnder interferometer. The optical input signal is preamplified before entering the interferometer, regulating the converted output signal by predominantly cross-phase modulation in the SOA of the arm of the MZI. This type of device has been used to demonstrate wavelength conversion over a range of input and output wavelengths [7]. Signal gain has also been shown to be possible.

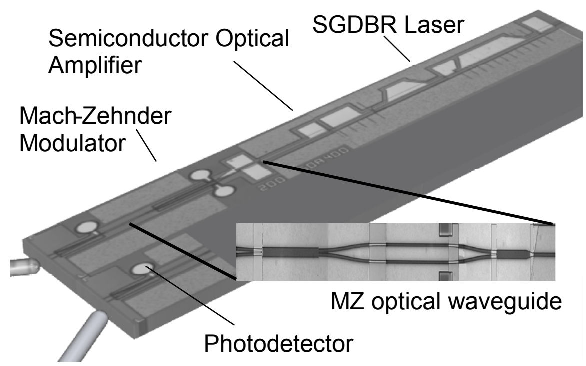

Fig. 7. MZ OE-O wavelength converter.

An alternative converter architecture is the OEIC wavelength converter. Here, the input optical signal is converted into an electrical signal that regulates the optical output signal. The added complexity from the added electrical path is compensated by the elimination of any need for optical filtering at the output, enabling same-wavelength conversion, and the capability of convenient signal monitoring. Figure 7 shows a schematic of an OEIC-WC, where the Mach-Zehnder is modulated by the unamplified photocurrent from a photodetector.

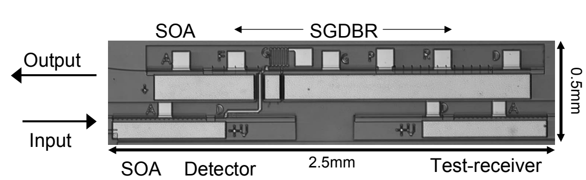

Fig. 8. Directly-modulated OE-O wavelength converter.

A second variety of an OEIC-WC is shown in Fig. 8. Here, the SG-DBR laser is directly modulated by the detector photocurrent. An input and output SOA is used to compensate for coupling and conversion losses. This type of device has the potential for high linearity, exploiting the relatively high linearity of direct modulation, compared to external modulation. However, ultimately the distortion produced in the input and output SOA should be eliminated to provide high linearity. One promising prospect is the use of series-connected multiple active regions in the SG-DBR laser. This kind of structure will recirculate the modulation current in the active region of the SG-DBR to provide enhanced direct modulation sensitivity that compensates for the coupling losses of the wavelength converter without the need for an SOA. In [8] this principle was used to demonstrate an equivalent 390% differential quantum efficiency of a Fabry-Perot type laser. In addition, the more uniform current distribution in such an active region has been shown to enhance linearity, compared to the corresponding single section device.

VI. Summary

The transmission of broadband and/or multiservice wireless signals over a WDM fiber network will put severe constraints on the allowable distortion produced in the optical link. Therefore, high performance optical components are needed to deliver the required link performance. Wavelength tunable integrated components based around Sampled-Grating DBR lasers are investigated for these purposes, in particular integrated high-performance analog transmitters based around EA- or MZ-modulators. Further, more complex devices enabling wavelength conversion in these kind of applications are also summarized.

Acknowledgements

This work was in part funded by DARPA/MTO under the RFLICS program and under the CS-WDM program.

References

[1] D. Wake, D, "Trends and prospects for radio over fibre picocells," *International Topical Meeting on Microwave Photonics*, pp. 21 -24, Nov 5-8, 2002.

[2] C. Lim, A. Nirmalathas, M. Attygalle, D. Novak, R. Waterhouse, "The merging of a WDM fiber-radio backbone with a 25 GHz WDM ring network*," 2003 IEEE MTT-S Microwave Symposium Digest*, vol.1, pp. 273 -276, June 8-1,3 2003.

[3] V. Jayaraman, Z.-M. Chuang, L. A. Coldren, "Theory, Design, and Performance of Extended Tuning Range Semiconductor Laser with Sampled Grating", *IEEE J. of Quantum Electron.*, **29**, pp. 1824 –1834, 1993.

[4] Y. A. Akulova, G. A. Fish, P. C. Koh, C. Schow, P. Kozodoy, A. Dahl, S. Nakagawa, M. Larson, M. Mack, T. Strand, C. Coldren, E. Hegblom, S. Penniman, T. Wipiejewski, and L. A. Coldren, "Widely-Tunable Electroabsorption-Modulated Sampled Grating DBR Laser Transmitter", *IEEE Journal on Selected Topics in Quantum Electronics.***8**, pp. 1349-1357, 2002.

[5] L.A. Johansson, Y.A. Akulova, G.A. Fish and L.A. Coldren, "Widely Tunable EAM-Integrated SGDBR Laser Transmitter for Analog Applications," *IEEE Photon. Technol. Lett.*, **15**, sep. 2003.

[6] J.S. Barton, E.J. Skogen, M.L. Masanovic, S.P. DenBaars and L.A. Coldren, "Tailorable chirp using integrated Mach-Zehnder modulators with tunable sampled grating distributed Bragg reflector lasers," *IEEE 18th International Semiconductor Laser Conference*, 2002. pp. 49-50.

[7] M.L. Masanovic, V. Lal, J.S. Barton, E.J. Skogen, L.A. Coldren, D.J. Blumenthal*, "*Monolithically integrated mach-Zehnder interferometer wavelength converter and widely tunable laser in InP," *IEEE Photon. Technol. Lett.* **15**, pp. 1117-1119, 2003.

[8] J. Getty, E. Skogen, L.A. Coldren, "Segmented 1.55um Laser with 400% Differential Quantum Efficiency," *Optical Fiber Communication Conference and Exhibit, 2002, TuG1.*